

## Exclusive/inclusive ratio of semileptonic $\Lambda_b$ decays

J. G. Körner\*

*Institut für Physik, Johannes Gutenberg-Universität, D-55099 Mainz, Germany*

B. Melić†

*Theoretical Physics Division, Rudjer Bošković Institute, P.O. Box 180, HR-10002 Zagreb, Croatia*

(Received 15 May 2000; published 6 September 2000)

We present theoretical evidence that the exclusive/inclusive ratio of semileptonic  $\Lambda_b$  decays exceeds that of semileptonic  $B$  decays where the experimental exclusive/inclusive ratio amounts to about 66%. We start from the observation that the spectator quark model provides a lower bound on the leading order Isgur-Wise function of the  $\Lambda_b \rightarrow \Lambda_c$  transition in terms of the corresponding  $B \rightarrow D, D^*$  mesonic Isgur-Wise function. Using experimental data for the  $B \rightarrow D, D^*$  mesonic Isgur-Wise functions this bound is established. Applying a Bethe-Salpeter model including spectator quark interactions and a QCD sum rule estimate of the  $\Lambda_b \rightarrow \Lambda_c$  transition form factor which satisfy the spectator quark model bound we predict the exclusive/inclusive ratio of semileptonic  $\Lambda_b$  decay rates to lie in a range between 0.81 and 0.92. We also provide an upper bound on the baryonic Isgur-Wise function which is determined from the requirement that the exclusive rate should not exceed the inclusive rate.

PACS number(s): 14.20.Mr, 13.30.Ce

### I. INTRODUCTION

In mesonic semileptonic  $b \rightarrow c$  transitions, the exclusive transitions to the ground state  $S$ -wave mesons  $B \rightarrow D, D^*$  make up approximately 66% of the total semileptonic  $B \rightarrow X_c$  rate [1]. It would then be interesting to know what the corresponding semileptonic rate ratio  $\Gamma_{\Lambda_b \rightarrow \Lambda_c} / \Gamma_{\Lambda_b \rightarrow X_c}$  (termed  $R_E$  in the following) is in semileptonic  $\Lambda_b$  decays. This is an important experimental issue since knowledge of this ratio would greatly facilitate the analysis of semileptonic  $\Lambda_b$  decays. For example, if the semileptonic  $\Lambda_b$  decays were dominated by the quasielastic exclusive channel  $\Lambda_b \rightarrow \Lambda_c + l^- + \bar{\nu}_l$ , this would be of considerable help in the kinematical reconstruction of their decays inasmuch as the  $\Lambda_c$  baryon is easy to detect via its decay mode  $\Lambda_c \rightarrow p K^- \pi^+$ . Unfortunately nothing is known experimentally about this ratio yet.

In this paper we attempt to address the problem of determining the exclusive/inclusive ratio  $R_E$  in semileptonic  $\Lambda_b$  decays from a theoretical point of view by consulting some model calculations which we critically scrutinize. We also attempt to extrapolate from the experimentally known results in the meson sector to the baryon sector.

As concerns the inclusive semileptonic rates of bottom mesons and bottom baryons one is now reasonably confident that they can be reliably calculated using the usual operator product expansion within heavy quark effective theory (HQET). The leading term in the operator product expansion (OPE) is given by the free heavy quark decay rate which clearly is the same for baryons and mesons. Radiative corrections to the free quark decay rate are quite large but again are identical for mesons and baryons. Differences in the inclusive semileptonic rates of mesons and the  $\Lambda_b$  baryon set

in only at  $\mathcal{O}(1/m_b^2)$ . They affect the mesonic and  $\Lambda_b$  rates differently since there is no chromomagnetic  $\mathcal{O}(1/m_b^2)$  correction in the  $\Lambda_b$  case. However, since the chromomagnetic term contributes only at the 3.7% level, the difference in the inclusive semileptonic rates for mesons and baryons is predicted to be quite small.

A much more difficult task is to get a reliable theoretical handle on the quasielastic exclusive semileptonic  $\Lambda_b \rightarrow \Lambda_c$  rate. There exist a number of theoretical calculations on the exclusive decay  $\Lambda_b \rightarrow \Lambda_c + l^- + \bar{\nu}_l$  using various model assumptions. They are of no great help since their predicted rate values may differ by factors of up to 3 and it is not easy to judge the reliability of the various model assumptions that enter the calculation. Ideally one would like to have model calculations that are valid both in the heavy meson and the heavy baryon sector. If these model calculations give sensible results in the heavy meson sector, where they can be checked against data, one would have more confidence in their predictions for the heavy baryon sector.

The paper is structured as follows. In Sec. II we take a first look at the leading order rate formula for the exclusive semileptonic decays of  $B$  mesons and  $\Lambda_b$  baryons in order to get a semiquantitative handle on the relative size of their rates. The analysis is refined in Sec. III for  $\Lambda_b$  baryons where  $1/m_b$  and  $1/m_b^2$  corrections and renormalization effects are included. In Sec. IV we recapitulate the calculation of the semileptonic inclusive decay rates. The results of the Secs. III and IV are brought together in Sec. V where we discuss the exclusive/inclusive ratio  $R_E$  of semileptonic  $\Lambda_b$  decays. We present numerical results on the exclusive/inclusive ratio for various models and give our best estimate of this ratio. In Sec. VI we classify the possible nonexclusive final states that will have to fill the gap between the exclusive and inclusive rates in semileptonic  $\Lambda_b$  decays. Section VII, finally, contains our conclusions.

### II. HEAVY QUARK LIMIT

For a quick first appraisal of the question of how the exclusive semileptonic decays of mesons and baryons are

\*Email: koerner@thep.physik.uni-mainz.de

†Email: melic@thphys.irb.hr

related we turn to the heavy quark limit and list the leading order semileptonic rate formulas for the  $B \rightarrow (D + D^*)$  and  $\Lambda_b \rightarrow \Lambda_c$  transitions. One has [1,2]

$$\frac{d\Gamma \left\{ \begin{array}{l} \text{meson} \\ \text{baryon} \end{array} \right\}}{d\omega} = \frac{G_F^2 |V_{bc}|^2 M_1^5}{12\pi^3} r^3 \sqrt{\omega^2 - 1} [3\omega(1+r^2) - 2r(2\omega^2 + 1)] \left\{ \begin{array}{l} \frac{\omega+1}{2} |F_{\text{meson}}(\omega)|^2 \\ |F_{\text{baryon}}(\omega)|^2 \end{array} \right\}, \quad (2.1)$$

where  $r = M_2/M_1$  and  $\omega = (M_1^2 + M_2^2 - q^2)/2M_1M_2$ . Here  $F_{\text{meson}}(\omega)$  and  $F_{\text{baryon}}(\omega)$  are the leading order Isgur-Wise transition form factors for the  $B \rightarrow D, D^*$  and  $\Lambda_b \rightarrow \Lambda_c$  transitions, respectively. Throughout the paper we refer to  $M_1$  and  $M_2$  as the masses of the initial and final particles in the semileptonic decay process.

The free heavy quark decay rate (or leading order parton model rate) which we need later on is simply obtained by replacing the particle masses in Eq. (2.1) by the corresponding quark masses and setting the curly brackets in Eq. (2.1) to 1, i.e., by taking the current coupling in the  $\Lambda_b \rightarrow \Lambda_c$  case to be point like. We shall encounter the integrated parton model rate for the  $\Lambda_b \rightarrow \Lambda_c$  case again in Sec. IV. Finally, in the heavy quark limit one has to determine the final meson mass  $M_2$  by taking the weighted average  $\bar{M}_D = 1/4(M_D + 3M_{D^*}) = 1.973$  GeV with  $M_D = 1.869$  GeV and  $M_{D^*} = 2.010$  GeV. For the pseudoscalar bottom quark mass we take  $M_B = 5.279$  GeV. For the  $\Lambda_Q$ -baryon masses we use  $M_{\Lambda_b} = 5.624$  GeV and  $M_{\Lambda_c} = 2.285$  GeV.

When trying to compare the two rates in Eq. (2.1) one identifies two main determining factors which counteract each other. On the one hand, one has the form factor expressions in the curly brackets which tend to enhance the mesonic rate due to the multiplicative factor  $(\omega+1)/2$  in the mesonic case. Also, according to common prejudice the baryon form factor falls off more rapidly than the mesonic form factor. On the other hand, one has the overall mass factor  $M_1^5 r^3$  which enhances the baryonic rate because  $M_1^5 r^3 = 214.16$  GeV<sup>5</sup> and  $M_1^5 r^3 = 377.37$  GeV<sup>5</sup> in the mesonic and baryonic cases, respectively.

It is evident that the choice of mesonic and baryonic Isgur-Wise functions plays a crucial role when comparing the two rates. As has been emphasized before, there exists some experimental knowledge on the mesonic Isgur-Wise function but nothing is known experimentally about the baryonic Isgur-Wise function yet.<sup>1</sup>

<sup>1</sup>The only available experimental result is from a preprint version of a DELPHI analysis [3]. This paper quotes a value of  $\rho^2 = 1.81_{-0.67}^{+0.70} \pm 0.32$  for the slope of the baryonic Isgur-Wise function. However, since this paper has never been published, we shall not use their result in our analysis.

For quick reference it is sometimes convenient to characterize the falloff behavior of the Isgur-Wise functions by expanding it around the zero recoil point where one has the zero recoil normalization condition  $F(1) = 1$ . Keeping terms up to second order in this expansion one has

$$F(\omega) = F(1)[1 - \rho^2(\omega - 1) + c(\omega - 1)^2 + \dots], \quad (2.2)$$

where the coefficients  $\rho^2$  and  $c$  are called the slope parameter and the convexity parameter, respectively. The slope parameter is frequently used to characterize the falloff behavior of the Isgur-Wise function. The expansion (2.2) is useful if one studies the physics close to zero threshold but may give misleading results when calculating rates because the spectral weight function multiplying the form factor functions is essentially determined by the square root factor  $\sqrt{\omega^2 - 1}$  in Eq. (2.1) and is therefore strongly weighted towards the end of the spectrum. It goes without saying that the slope and convexity parameters are in general different for the mesonic and baryonic Isgur-Wise functions.

In order to proceed with our first appraisal of the magnitude of the exclusive mesonic and baryonic semileptonic rates we appeal to the spectator quark model where the mesonic and baryonic Isgur-Wise functions become related to one another [2,4]. In the spectator quark model one has

$$F_{\text{baryon}}(\omega) = \frac{\omega+1}{2} |F_{\text{meson}}(\omega)|^2. \quad (2.3)$$

Explicit calculations show that the baryonic form factor is considerably underestimated by the spectator relation (2.3). Nevertheless, the spectator relation (2.3) may still serve as an effective lower bound on the baryonic form factor.

The physical picture behind the spectator quark model relation is quite simple. In the heavy baryon case there are two light spectator quarks that need to be accelerated in the current transition compared to the one spectator quark in the heavy meson transition. Thus the baryonic form factor is determined in terms of the square of the mesonic form factor. The factor  $[(\omega+1)/2]$  is a relativistic factor which ensures the correct threshold behavior of the baryonic form factor in the crossed  $e^+e^-$  channel [2,4].

In [4] the relation between heavy meson and heavy baryon form factors was investigated in the context of a dynamical Bethe-Salpeter (BS) model. The above spectator quark model relation (2.3) in fact emerges when the interaction between the light quarks in the heavy baryon is switched off in the BS interaction kernel. In the more realistic situation when the light quarks interact with each other, the heavy baryon form factor becomes flatter; i.e., the spectator quark model form factor may be used to bound the heavy baryon form factor from below. In Fig. 1 we reproduce from [4] the  $\omega$  dependence of the spectator quark model form factor and that of two representative form factors with the interaction between the light quarks included. The starting point in [4] is a mesonic form factor with a slope of  $\rho_{\text{meson}}^2 = 1$  which, according to Eq. (2.3), leads to a spectator form factor with a slope of  $\rho_{\text{baryon}}^2 = 1.5$ . The spectator form factor is the lowest form factor shown in Fig. 1. The interaction between the

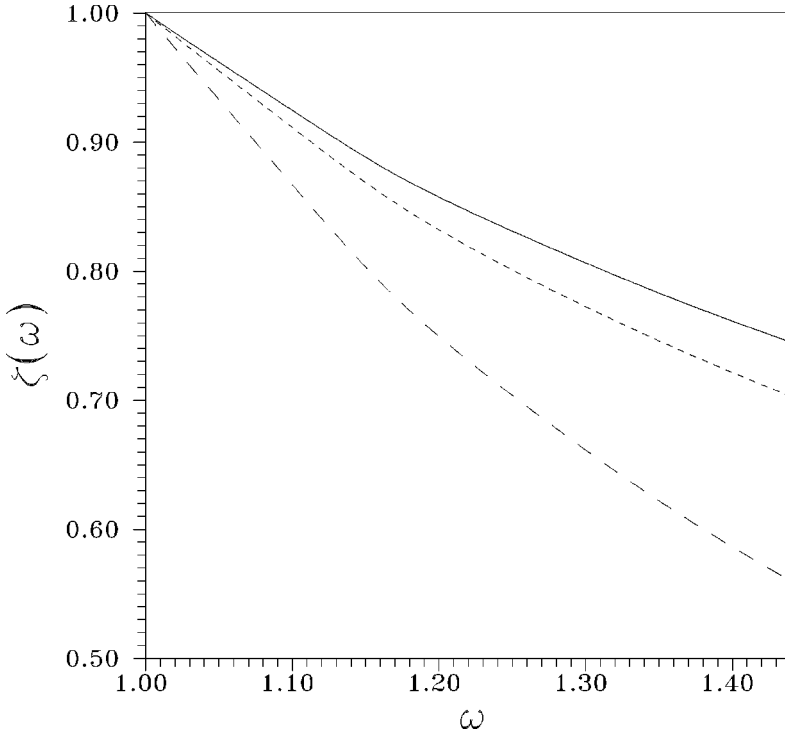


FIG. 1. Leading order baryon form factor  $F_{\text{baryon}}(\omega)$  in the dynamic Bethe-Salpeter model of [4] (denoted by  $\zeta(\omega)$  in this figure). (a) Non-interacting light quarks (long-dashed line) and (b) interacting light quarks with the range parameter  $\Lambda_B = 500$  MeV (solid line) and  $\Lambda_B = 355$  MeV (short-dashed line).

light quarks was introduced through a harmonic oscillator type kernel in the BS equation. The two upper form factor curves in Fig. 1 correspond to two different choices of the oscillator strength with which the light quarks interact or, equivalently, correspond to two different choices of the size parameter in the oscillator wave function. The interaction type form factors in Fig. 1 have slopes of  $\rho_{\text{baryon}}^2 = 0.81$  (solid line) and  $0.97$  (short-dashed line) [4]. They are considerably flatter than the spectator quark model form factor.

We shall now calculate exclusive rates for mesonic and baryonic transitions according to Eq. (2.1) using the spectator model relation (2.3). According to what was said before, the baryonic rate calculated in this way must subsequently be adjusted upward according to the analysis of [4]. We went to considerable lengths in explaining the results of [4] because we want to emphasize that the outcome of the baryonic rate estimate using the spectator quark model relation (2.3) must be viewed as providing only lower bounds on the true quasi-elastic baryonic rate. For the mesonic form factor we use the world average of the slope  $\rho_{\text{meson}}^2$  obtained by combining results from  $B \rightarrow D^*$  and  $B \rightarrow D$  transitions,  $\rho_{\text{meson}}^2 = 0.70$  [5].<sup>2</sup> Using  $V_{cb} = 0.038$ , a linear meson form factor with the above slope, a baryonic form factor according to the spectator relation (2.3) and the rate formulas (2.1) one obtains  $\Gamma_{\text{meson}} = 5.30 \times 10^{10} \text{ s}^{-1}$  and  $\Gamma_{\text{baryon}} = 5.04 \times 10^{10} \text{ s}^{-1}$ . As has been emphasized before the baryonic rate  $\Gamma_{\text{baryon}} = 5.04 \times 10^{10} \text{ s}^{-1}$  has to be adjusted upward in the more realistic situation of interacting light quarks. Looking at the model calculation [4] for guidance, the increment in rate going from

noninteracting (spectator) to interacting quarks is 1.28 and 1.37, respectively, for the two choices of oscillator strengths analyzed in [4]. Adjusting the above baryonic rate accordingly our leading order estimate of the baryonic rate is thus  $\Gamma_{\text{baryon}} = (6.45 - 6.90) \times 10^{10} \text{ s}^{-1}$ . Starting from a mesonic exclusive/inclusive ratio of 66% and assuming equal inclusive semileptonic rates for bottom baryons and mesons, which is sufficiently accurate for our semiquantitative calculation, our estimate for the exclusive/inclusive ratio in semileptonic  $\Lambda_b$  decays is  $R_E = (80 - 86)\%$ . This is considerably larger than the mesonic exclusive/inclusive ratio  $R_E \approx 66\%$ .

Up to this point our semiquantitative analysis was done to leading order in HQET. How would finite mass effects affect our previous conclusions? One way of improving the previous analysis in the meson sector is to insert physical masses in the rate expression (2.1), thereby including part of the  $1/m_Q$  corrections to Eq. (2.1). To do this we need to disentangle the  $B \rightarrow D$  and  $B \rightarrow D^*$  rates in Eq. (2.1). One has [1]

$$\frac{d\Gamma(B \rightarrow D)}{d\omega} = \frac{G_F^2 |V_{bc}|^2 M_1^5}{48\pi^3} \times r^3 (1+r)^2 (\omega^2 - 1)^{3/2} |F_{\text{meson}}(\omega)|^2 \quad (2.4)$$

and

$$\frac{d\Gamma(B \rightarrow D^*)}{d\omega} = \frac{G_F^2 |V_{bc}|^2 M_1^5}{48\pi^3} r^3 \sqrt{\omega^2 - 1} \times (\omega + 1) [(1-r)^2 (\omega + 1) + 4\omega(1 - 2\omega r + r^2)] |F_{\text{meson}}(\omega)|^2. \quad (2.5)$$

<sup>2</sup>The CLEO Collaboration also attempted a linear plus quadratic fit to the data, but the data were not good enough to determine the convexity parameter  $c$  of the meson form factor with any accuracy.

Using now the world average of  $(\rho_{\text{meson}}^2)^{B \rightarrow D} = 0.66$  and  $(\rho_{\text{meson}}^2)^{B \rightarrow D^*} = 0.71$  with linear form factors and taking physical  $D$  and  $D^*$  masses one finds  $\Gamma_{B \rightarrow D} = 1.39 \times 10^{10} \text{ s}^{-1}$  and  $\Gamma_{B \rightarrow D^*} = 3.90 \times 10^{10} \text{ s}^{-1}$ , giving a total mesonic rate of  $\Gamma_{B \rightarrow D+D^*} = 5.30 \times 10^{10} \text{ s}^{-1}$ . It fully agrees with the above result and therefore leaves the foregoing conclusions intact.

Continuing with our discussion on the contributions of nonleading effects in the  $1/m_Q$  expansion we now turn to results of some model calculations in order to find out how nonleading effects may affect the above conclusions. In the mesonic sector Neubert and Rieckert [6] analyzed an infinite momentum frame model and found that  $\mathcal{O}(1/m_Q)$  effects raise the  $B \rightarrow D$  and  $B \rightarrow D^*$  rates by 15.7% and 0.5%, respectively, resulting in a rise of 4.4% for the total  $D+D^*$  rate. Using a similar infinite momentum frame model König *et al.* find that the  $\mathcal{O}(1/m_Q)$  effects raise the semileptonic  $\Lambda_b \rightarrow \Lambda_c$  rate by 3% [7] which is quite close to the 4.4% found in [6] in the bottom meson case. Judging from these model calculations our leading order comparison of the mesonic and baryonic rates and the conclusions drawn from it do not seem to be much affected by  $\mathcal{O}(1/m_Q)$  corrections.

There also exist estimates of  $\mathcal{O}(1/m_Q^2)$  corrections in the literature. Faustov and Galkin use a relativistic quark model based on the quasipotential approach [8]. They quote exclusive/inclusive branching ratios of  $(13.5+3.3-1.4)\%$  and  $(39.1+6.5-3.9)\%$  for semileptonic  $B \rightarrow D$  and  $B \rightarrow D^*$  rates, where the second and third numbers refer to the  $\mathcal{O}(1/m_Q)$  and  $\mathcal{O}(1/m_Q^2)$  corrections, respectively. The  $\mathcal{O}(1/m_Q)$  corrections in this model are considerably larger than in the infinite momentum frame models. Ivanov *et al.* investigated the role of finite mass effects in semileptonic  $\Lambda_b \rightarrow \Lambda_c$  decays without taking recourse to the heavy mass expansion. They found an overall rate reduction of 9% relative to the infinite mass result [9]. In the analysis of the present paper presented in Sec. III we obtain  $\approx +5\%$  and  $\approx -7\%$  for the  $\mathcal{O}(1/m_Q)$  and  $\mathcal{O}(1/m_Q^2)$  corrections to the  $\Lambda_b \rightarrow \Lambda_c$  decays, respectively. From all these model calculations one learns that the  $\mathcal{O}(1/m_Q)$  corrections tend to increase the rates whereas the  $\mathcal{O}(1/m_Q^2)$  corrections tend to decrease the rates, for both heavy meson and heavy baryon decays. Again, our leading order estimate of the relative size of the exclusive/inclusive ratios of bottom mesons and baryons is not likely to be affected much by including also  $\mathcal{O}(1/m_Q^2)$  effects. The same holds true for renormalization effects of the weak current which affect the bottom baryon and bottom meson amplitudes equally and therefore drop out in the ratio of exclusive semileptonic bottom meson and baryon decays.

The conclusion drawn in this section on the predominance of the exclusive/inclusive ratio of semileptonic  $\Lambda_b$  decays over that of semileptonic  $B$  decays carries over to the more sophisticated analysis of the next sections where we include  $1/m_Q$  and  $1/m_Q^2$  effects, and radiative corrections.

### III. EXCLUSIVE SEMILEPTONIC RATE $\Lambda_b \rightarrow \Lambda_c + l^- + \bar{\nu}_l$

It is most convenient to represent the differential decay rate in terms of the helicity amplitudes of the process. One

has (we take leptons to be massless) [2,10]

$$\frac{d\Gamma(\Lambda_b \rightarrow \Lambda_c)}{d\omega} = \frac{G_F^2 |V_{bc}|^2 q^2 M_2^2 \sqrt{\omega^2 - 1}}{96\pi^3 M_1} (|H_{1/2,1}|^2 + |H_{-1/2,-1}|^2 + |H_{1/2,0}|^2 + |H_{-1/2,0}|^2). \quad (3.1)$$

The helicity amplitudes are in turn related to the invariant amplitudes of the process via

$$\begin{aligned} \sqrt{q^2} H_{1/2,0}^{V,A} &= \sqrt{2M_1 M_2 (\omega \mp 1)} [(M_1 \pm M_2) f_1^{V,A} \\ &\quad \pm M_2 (\omega \pm 1) f_2^{V,A} \pm M_1 (\omega \pm 1) f_3^{V,A}], \\ H_{1/2,1}^{V,A} &= -2\sqrt{M_1 M_2 (\omega \mp 1)} f_1^{V,A}, \end{aligned} \quad (3.2)$$

where the invariant amplitudes are defined by

$$\begin{aligned} \langle \Lambda_c(v_2) | J_\mu^V | \Lambda_b(v_1) \rangle &= \bar{u}_c(v_2) (f_1^V \gamma_\mu + f_2^V v_{1\mu} \\ &\quad + f_3^V v_{2\mu}) u_b(v_1), \\ \langle \Lambda_c(v_2) | J_\mu^A | \Lambda_b(v_1) \rangle &= \bar{u}_c(v_2) (f_1^A \gamma_\mu + f_2^A v_{1\mu} \\ &\quad + f_3^A v_{2\mu}) \gamma_5 u_b(v_1). \end{aligned} \quad (3.3)$$

The total helicity amplitudes finally are given by

$$H_{\lambda_2, \lambda_W} = H_{\lambda_2, \lambda_W}^V - H_{\lambda_2, \lambda_W}^A, \quad (3.4)$$

where the choice of the relative minus sign between the vector and axial vector helicity amplitudes reflects the  $(V-A)$  structure of the  $b \rightarrow c$  current transition. The  $H_{\lambda_2, \lambda_W}^{V,A}$  are the helicity amplitudes for the vector (V) and axial-vector (A) current-induced transition in the decay  $1/2^+ \rightarrow 1/2^+ + W_{\text{off-shell}}^-$  with  $\lambda_2$  and  $\lambda_W$  being the helicities of the final state baryon and the  $W$  boson, respectively.

The remaining helicity amplitudes are related to the above helicity amplitudes (3.2) by parity. One has

$$H_{-\lambda_2, -\lambda_W}^{V,A} = \pm H_{\lambda_2, \lambda_W}^{V,A}. \quad (3.5)$$

It is well known that the complexity of the form factor structure exemplified by the set of six form factors  $f_i^{V,A}$  ( $i=1,2,3$ ) is considerably reduced in HQET. Working up to  $\mathcal{O}(1/m_Q)$  in HQET and including also  $\mathcal{O}(\alpha_s)$  corrections one finds [2]

$$\begin{aligned} f_1^V(\omega) &= F(\omega) + \left( \frac{1}{2M_1} + \frac{1}{2M_2} \right) [\eta(\omega) + \bar{\Lambda}F(\omega)] \\ &\quad + \frac{\alpha_s(\bar{m})}{\pi} v_1(\omega, \lambda) F(\omega), \end{aligned} \quad (3.6)$$

$$f_2^V(\omega) = F(\omega) \left( -\frac{1}{M_2} \frac{1}{\omega+1} \bar{\Lambda} - \frac{\alpha_s(\bar{m})}{\pi} v_2(\omega) \right),$$

$$f_3^V(\omega) = F(\omega) \left( -\frac{1}{M_1} \frac{1}{\omega+1} \bar{\Lambda} - \frac{\alpha_s(\bar{m})}{\pi} v_3(\omega) \right),$$

$$f_1^A(\omega) = F(\omega) + \left( \frac{1}{2M_1} + \frac{1}{2M_2} \right) \left( \eta(\omega) + \bar{\Lambda} F(\omega) \frac{\omega-1}{\omega+1} \right) + \frac{\alpha_s(\bar{m})}{\pi} a_1(\omega, \lambda) F(\omega),$$

$$f_2^A(\omega) = F(\omega) \left( -\frac{1}{M_2} \frac{1}{\omega+1} \bar{\Lambda} - \frac{\alpha_s(\bar{m})}{\pi} a_2(\omega) \right),$$

$$f_3^A(\omega) = F(\omega) \left( \frac{1}{M_1} \frac{1}{\omega+1} \bar{\Lambda} - \frac{\alpha_s(\bar{m})}{\pi} a_3(\omega) \right).$$

The  $\mathcal{O}(\alpha_s)$  corrections to the form factors have been taken from [11]. They result from the  $\mathcal{O}(\alpha_s)$  vertex correction to the current-induced  $b \rightarrow c$  transition [12]. The infrared singularity is regularized by the introduction of a fictitious gluon mass which is taken to be  $\lambda = 0.2$  GeV. At zero recoil, where the vertex correction is infrared finite, the renormalization is independent of the gluon mass regulator. However, away from zero recoil, the  $\alpha_s$ -correction functions  $v_1(\omega, \lambda)$  and  $a_1(\omega, \lambda)$  depend on the gluon mass regulator. This introduces a certain amount of model dependence in the renormalization procedure. The above value of the gluon mass was chosen according to the expectation that the exchange of virtual gluons in the vertex correction should be cut off at frequencies  $k^0 \sim 1/R$  with  $R \sim 1$  fm being a typical hadronic scale. The argument of the  $\alpha_s$  coupling,  $\bar{m}$ , is taken such that effects of higher order terms  $[\alpha_s \ln(m_b/m_c)]^n$  are minimized,  $\bar{m} = 2m_b m_c / (m_b + m_c) \simeq 2.31$  GeV. In this way one avoids the use of the renormalization-group-improved summation of leading logarithms, which has been proven as inconsistent [11].

The binding energy of the  $\Lambda_b$  is denoted by  $\bar{\Lambda}$  which we take to be 0.6 GeV. The form factor function  $\eta(x)$  results from the nonlocal contribution of the kinetic energy term of the  $1/m_Q$  corrected HQET Lagrangian. It has been calculated in two different model approaches and has found to be negligibly small [7,13]. Therefore, we can safely drop its contribution in the following. By neglecting the form factor  $\eta(x)$  in the  $\mathcal{O}(1/m_Q)$  result (3.6) the differential rate (3.1) is proportional to the square of the leading order Isgur-Wise function  $F(\omega)$  with its zero recoil normalization  $F(1) = 1$ . In this way we can meaningfully compare our results with the leading order results of other model calculations as will be done in Sec. V.

It is well known that  $\mathcal{O}(1/m_Q^2)$  corrections to the unit zero recoil normalization of Isgur-Wise functions can be substantial. For example, by evaluating zero recoil sum rules, the authors of Ref. [14] obtain

$$F(1)_{B \rightarrow D} = 0.98 \pm 0.07,$$

$$F(1)_{B \rightarrow D^*} = 0.91 \pm 0.03, \quad (3.7)$$

in the mesonic case. In the  $\Lambda_b \rightarrow \Lambda_c$  case the zero recoil sum rule gives a bound on the zero recoil value of the sole remaining form factor function  $f_1^A$ . The (unrenormalized) zero recoil sum rule leads to  $f_1^A(1) \leq (1 - 0.165 \mu_\pi^2 / \text{GeV}^2)^{1/2}$  [15]. Using  $\mu_\pi^2 = 0.5 \text{ GeV}^2$  [18,19],  $f_1^A(1)$  must be smaller than 0.958. For definiteness we take a value close to the upper bound:

$$f_1^A(1) = 0.95. \quad (3.8)$$

This value is nicely corroborated by the finite heavy quark mass calculation of [9] where one finds  $f_1^A(1) = 0.97$ .

Nothing is known about the size of the  $\mathcal{O}(1/m_Q^2)$  corrections to  $\Lambda_b \rightarrow \Lambda_c$  away from zero recoil, except that they can be parametrized in terms of ten new  $\omega$ -dependent form factors and one new dimensionful constant [16], the magnitude and functional forms of which are not known. The lack of knowledge about the  $\mathcal{O}(1/m_Q^2)$  corrections away from zero recoil prevents us from their exact treatment. On the other hand, the size of the  $\mathcal{O}(1/m_Q^2)$  correction at zero recoil is a clear indication that the  $\mathcal{O}(1/m_Q^2)$  corrections cannot be neglected. We shall therefore adopt the following strategy. We smoothly extrapolate from the  $\mathcal{O}(1/m_Q^2)$  information at zero recoil to the whole  $\omega$  range. The appropriate amplitude for this extrapolation is the axial vector current  $S$ -wave amplitude, the zero recoil value of which is determined by the zero recoil sum rules. We thus multiply the axial-vector-current  $S$ -wave amplitude everywhere by its zero recoil value  $f_1^A(1) = 0.95$ . It is clear that the  $\mathcal{O}(1/m_Q^2)$  corrections at zero recoil are exactly included in this approach. The lack of knowledge about the  $\mathcal{O}(1/m_Q^2)$  corrections to the other partial-wave amplitudes leaves us no choice but to leave them untreated. With this in mind it is gratifying to note that the  $S$ -wave contribution dominates the quasielastic rate. For example, using the standard form factor (5.1) with  $\rho_B^2 = 0.75$  in a leading order calculation one finds that the  $S$ -wave contribution amounts to  $\simeq 66\%$  of the total semileptonic rate.

In order to set up our procedure of how to incorporate the  $\mathcal{O}(1/m_Q^2)$  corrections we define the relevant vector current (V) and axial vector current (A) partial-wave amplitudes  $A_{L,S}^{V,A}$  in terms of the helicity amplitudes  $H_{\lambda_2, \lambda_W}^{V,A}$ . Here  $L$  denotes the orbital angular momentum of the final state and  $S = J_{\text{current}} + S_{\Lambda_c}$  is the sum of the final state spin angular momenta where  $J_{\text{current}} = 1$  in the zero lepton mass case that we are considering here. One has

$$A_{1,1/2}^V = -\sqrt{\frac{2}{3}} H_{1/2,0}^V - \sqrt{\frac{4}{3}} H_{1/2,1}^V, \quad (3.9)$$

$$A_{2,3/2}^V = -\sqrt{\frac{4}{3}} H_{1/2,0}^V + \sqrt{\frac{2}{3}} H_{1/2,1}^V,$$

$$A_{0,1/2}^A = \sqrt{\frac{2}{3}} H_{1/2,0}^A - \sqrt{\frac{4}{3}} H_{1/2,1}^A,$$

$$A_{2,3/2}^A = \sqrt{\frac{4}{3}} H_{1/2,0}^A + \sqrt{\frac{2}{3}} H_{1/2,1}^A.$$

$$A_{0,1/2}^A \rightarrow f_1^A(1) A_{0,1/2}^A = A_{0,1/2}^A + (f_1^A(1) - 1) A_{0,1/2}^A. \quad (3.10)$$

By substituting invariant form factors according to Eqs. (3.2) one can verify the correct threshold behavior of the partial-wave amplitudes, i.e.,  $A_{1,1/2}^V, A_{1,3/2}^V \sim (\omega - 1)^{1/2}$ ,  $A_{0,1/2}^A \sim (\omega - 1)^0$  and  $A_{2,3/2}^A \sim (\omega - 1)^1$ .

According to the above strategy we now incorporate the  $\mathcal{O}(1/m_Q^2)$  corrections by multiplying the  $S$ -wave amplitude  $A_{0,1/2}^A$  by the  $\mathcal{O}(1/m_Q^2)$  zero recoil correction  $f_1^A(1) = 0.95$ . Thus we write

For the first term on the right-hand side (RHS) of Eq. (3.10) we substitute the  $\mathcal{O}(1/m_Q)$  result according to Eqs. (3.6). Contrary to this we use only the leading order result for  $A_{0,1/2}^A$  in the second term of Eq. (3.10) since it is already being multiplied by the  $\mathcal{O}(1/m_Q^2)$  factor  $[f_1^A(1) - 1]$ . Including also the  $A_{2,3/2}^A$  partial-wave amplitude the leading order expressions for the axial-vector partial-wave amplitudes read

$$\begin{aligned} A_{0,1/2}^A &= \frac{1}{\sqrt{q^2}} \frac{2}{\sqrt{3}} \sqrt{M_1 M_2 (\omega + 1)} F(\omega) \left[ (M_1 - M_2 + 2\sqrt{q^2}) \left( 1 + \frac{\alpha_s(\bar{m})}{\pi} a_1(\omega, \lambda) \right) - \frac{\alpha_s(\bar{m})}{\pi} (\omega - 1) [M_2 a_2(\omega) + M_1 a_3(\omega)] \right], \\ A_{2,3/2}^A &= \frac{1}{\sqrt{q^2}} \frac{2\sqrt{2}}{\sqrt{3}} \sqrt{M_1 M_2 (\omega + 1)} F(\omega) \left[ (M_1 - M_2 - \sqrt{q^2}) \left( 1 + \frac{\alpha_s(\bar{m})}{\pi} a_1(\omega, \lambda) \right) - \frac{\alpha_s(\bar{m})}{\pi} (\omega - 1) [M_2 a_2(\omega) + M_1 a_3(\omega)] \right]. \end{aligned} \quad (3.11)$$

Putting everything together we arrive at the differential rate. One obtains

$$\begin{aligned} \frac{d\Gamma(\Lambda_b \rightarrow \Lambda_c)}{d\omega} &= \frac{G_F^2 |V_{bc}|^2}{48\pi^3} \frac{q^2 M_2^2 \sqrt{\omega^2 - 1}}{M_1} \left\{ |H_{1/2,1}^V|^2 + |H_{1/2,0}^V|^2 + |H_{1/2,1}^A|^2 + |H_{1/2,0}^A|^2 \right. \\ &\quad + ([f_1^A(1)]^2 - 1) \frac{2}{3} \frac{M_1 M_2}{q^2} (\omega + 1) F^2(\omega) (M_1 - M_2 + 2\sqrt{q^2}) \\ &\quad \left. \times \left[ (M_1 - M_2 + 2\sqrt{q^2}) \left( 1 + 2 \frac{\alpha_s(\bar{m})}{\pi} a_1(\omega, \lambda) \right) - 2 \frac{\alpha_s(\bar{m})}{\pi} (\omega - 1) [M_2 a_2(\omega) + M_1 a_3(\omega)] \right] \right\}. \end{aligned} \quad (3.12)$$

In Eq. (3.12) the first line incorporates the  $\mathcal{O}(1)$  and  $\mathcal{O}(1/m_Q)$  contributions including the radiative corrections as specified by Eqs. (3.2) and (3.6). The second and third lines comprise the  $\mathcal{O}(1/m_Q^2)$  corrections (including radiative corrections) as described before. Since our aim is to compare our exclusive rate with the inclusive  $\mathcal{O}(\alpha_s)$  rate written down in Sec. IV, we have only retained radiative corrections up to  $\mathcal{O}(\alpha_s)$  in the exclusive rate (3.12) for consistency reasons.

For the sake of completeness we separately list the  $\mathcal{O}(1/m_Q^2)$  zero recoil corrections for the longitudinal and transverse pieces of the axial-vector contributions. They are needed for the transverse-longitudinal separation shown in Fig. 2. One has

$$\begin{aligned} |H_{1/2,0}^A|^2 &\rightarrow |H_{1/2,0}^A|^2 + \{[f_1^A(1)]^2 - 1\} \frac{1}{6} (A_{0,1/2}^A)^2 \\ &\quad + \sqrt{\frac{2}{9}} [f_1^A(1) - 1] A_{0,1/2}^A \cdot A_{2,3/2}^A, \end{aligned} \quad (3.13)$$

$$\begin{aligned} |H_{1/2,1}^A|^2 &\rightarrow |H_{1/2,1}^A|^2 + \{[f_1^A(1)]^2 - 1\} \frac{1}{3} (A_{0,1/2}^A)^2 \\ &\quad - \sqrt{\frac{2}{9}} [f_1^A(1) - 1] A_{0,1/2}^A \cdot A_{2,3/2}^A. \end{aligned}$$

When summing the two contributions (3.13) in the rate formula the  $A_{0,1/2}^A \cdot A_{2,3/2}^A$  interference contributions cancel out as is apparent in Eq. (3.12). As explained before we shall use the leading order results (3.11) for the second and third term in Eqs. (3.13) since the factors  $\{[f_1^A(1)]^2 - 1\}$  and  $[f_1^A(1) - 1]$  multiplying them are already of  $\mathcal{O}(1/m_Q^2)$ .

Our numerical evaluation of Eq. (3.12) is based on the standard form factor (5.1) with  $\rho_B^2 = 0.75$  using again  $V_{bc} = 0.038$ . All parameters have been specified before. For the quasielastic rate we find  $\Gamma^{\text{excl}} = 5.52 \times 10^{10} \text{ s}^{-1}$ . The  $\mathcal{O}(1/m_Q)$  and  $\mathcal{O}(1/m_Q^2)$  corrections amount to +5.2% and -6.6%. The renormalization of the heavy quark current decreases the exclusive rate by 8.8%. In Fig. 2 we show a plot of the  $\omega$  spectrum of the quasielastic rate where we sepa-

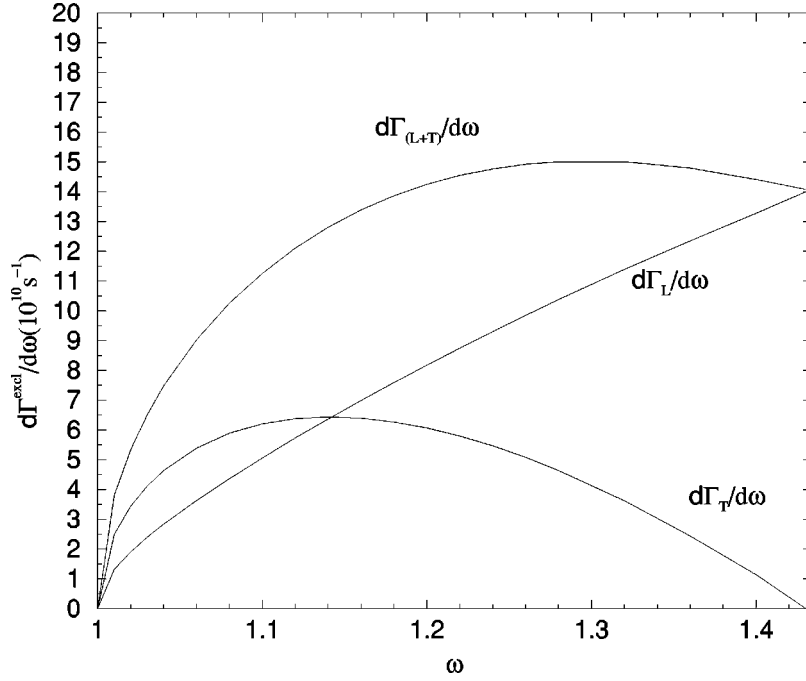


FIG. 2.  $\omega$  spectrum of the exclusive decay rate and partial rates of longitudinal and transversal transitions calculated with the standard form factor (5.1) using  $\rho_B^2=0.75$ .

rately show the transverse ( $\lambda_W = \pm 1$ ) and longitudinal contributions ( $\lambda_W = 0$ ) including  $\mathcal{O}(1/m_Q^2)$  and  $\mathcal{O}(\alpha_s)$  corrections calculated according to Eq. (3.13). The longitudinal rate dominates the spectrum except for a small region close to zero recoil. For the integrated rates we find  $\Gamma_L^{\text{excl}}/\Gamma_T^{\text{excl}} = 1.89$ .

#### IV. INCLUSIVE SEMILEPTONIC RATE $\Lambda_b \rightarrow X_c + l^- + \bar{\nu}_l$

To the leading order in the heavy mass expansion the inclusive rate is given by the free heavy quark decay rate which can be obtained from Eq. (2.1) using quark masses and setting the terms in the curly brackets equal to 1. There are no  $\mathcal{O}(1/m_Q)$  corrections to this result. Mass corrections come in at the order  $\mathcal{O}(1/m_Q^2)$ . In the case of  $\Lambda_b$  decay, where the light diquark system has spin 0, the chromomagnetic contribution drops out and the mass corrections are determined by the nonperturbative kinetic energy parameter

$\mu_\pi^2$  alone.

Including also the  $\alpha_s$  correction in the free quark decay rate [17], one has [ $x = (m_c/m_b)^2$ ]

$$\Gamma^{\text{incl}} = \Gamma_0 \left( 1 - \frac{2}{3} \frac{\alpha_s(m_b)}{\pi} g(x) \right) \left( 1 - \frac{\mu_\pi^2}{2m_b^2} \right), \quad (4.1)$$

where  $\Gamma_0$  is the lowest order (in  $\alpha_s$ ) free quark decay rate,

$$\Gamma_0 = \frac{G_F^2 |V_{bc}|^2 m_b^5}{192\pi^3} I_0(x), \quad (4.2)$$

$$I_0(x) = (1-x^2)(1-8x+x^2) - 12x^2 \ln x,$$

and the function  $g(x)$  is determined by the  $\mathcal{O}(\alpha_s)$  radiative corrections including all mass corrections as calculated in [17]:

$$g(x) = h(x)/I_0(x),$$

$$\begin{aligned} h(x) = & -(1-x^2) \left( \frac{25}{4} - \frac{239}{3}x + \frac{25}{4}x^2 \right) + x \ln(x) \left( 20 + 90x - \frac{4}{3}x^2 + \frac{17}{3}x^3 \right) + x^2 \ln^2(x) (36 + x^2) \\ & + (1-x^2) \left( \frac{17}{3} - \frac{64}{3} + \frac{17}{3}x^2 \right) \ln(1-x) - 4(1+30x^2+x^4) \ln(x) \ln(1-x) \\ & - (1+16x^2+x^4) [6\text{Li}_2(x) - \pi^2] - 32x^{3/2}(1+x) \left[ \pi^2 - 4\text{Li}_2(\sqrt{x}) + 4\text{Li}_2(-\sqrt{x}) - 2 \ln(x) \ln \left( \frac{1-\sqrt{x}}{1+\sqrt{x}} \right) \right]. \end{aligned} \quad (4.3)$$

The  $\mathcal{O}(1/m_b^2)$  corrections appear in the third factor of Eq. (4.1). For the value of the kinetic energy parameter  $\mu_\pi^2$  we take [18,19]

$$\mu_\pi^2 = 0.5 \text{ GeV}^2, \quad (4.4)$$

where we assume equality of the kinetic energy parameter in the meson and baryon case.

It is well known and evident from Eq. (4.2) that the inclusive decay rate depends rather strongly on the exact value of the  $b$ -quark mass  $m_b$  which is fraught with some uncertainties. We shall use the results of two recent theoretical analyses of the inclusive semileptonic decay rate. In [19] the value of  $m_b$  was determined from an analysis of  $Y$  sum rules and  $B$ -meson semileptonic widths:

$$m_b = 4.8 \text{ GeV}, \quad m_c = 1.325 \text{ GeV}, \quad (4.5)$$

where the charm quark mass was determined from the constraint

$$m_b - m_c - \mu_\pi^2 \left( \frac{1}{2m_c} - \frac{1}{2m_b} \right) = \bar{M}_B - \bar{M}_D. \quad (4.6)$$

The  $\bar{M}_{B,D}$  are the spin-averaged masses  $\bar{M}_{B,D} = 1/4(M_{B,D} + 3M_{B^*,D^*})$  as before.

In [20] the inclusive semileptonic  $B$  decay rate was directly expressed in terms of the  $Y(1S)$  meson mass instead of the  $b$  quark mass. The authors of [20] obtained

$$\Gamma^{\text{incl}-Y} = \frac{G_F^2 |V_{bc}|^2}{192\pi^3} \left( \frac{m_Y}{2} \right)^5 0.533 [1 - 0.096\epsilon - 0.029\epsilon^2 - (0.28\lambda_2 + 0.12\lambda_1)/\text{GeV}^2], \quad (4.7)$$

where  $\epsilon = 1$  denotes the order of the expansion in  $m_Y$ . Mass corrections and radiative corrections are already taken into account. The parameters  $\lambda_1$  and  $\lambda_2$  in Eq. (4.7) are connected with the more familiar  $\mu_\pi^2$  and  $\mu_G^2$  parameters by  $\mu_\pi^2 = -\lambda_1$  and  $\mu_G^2 = 3\lambda_2 = 0.36 \text{ GeV}^2$ . For the  $\Lambda_b$  baryon we set  $\lambda_2 = 0$  and assume equality of  $\lambda_1$  in the meson and baryon case as before.

For the semileptonic inclusive  $b \rightarrow c$  decay rate of the  $\Lambda_b$  we finally obtain  $\Gamma^{\text{incl}} = 6.50 \times 10^{10} \text{ s}^{-1}$  using the mass parameters from [19] and  $\Gamma^{\text{incl}-Y} = 6.23 \times 10^{10} \text{ s}^{-1}$  using the evaluation of [20]. Again we have set  $V_{bc} = 0.038$ . We mention that these two inclusive rate values include the  $\mathcal{O}(\alpha_s)$  radiative corrections which lower the inclusive rates by about 11%. This value is not very far away from the 8.8% by which the exclusive rate gets lowered by the same radiative corrections.

## V. EXCLUSIVE/INCLUSIVE $\Lambda_b \rightarrow \Lambda_c$ RATIO

In this section we determine the exclusive/inclusive ratio  $R_E = \Gamma^{\text{excl}}/\Gamma^{\text{incl}}$  in semileptonic  $\Lambda_b \rightarrow \Lambda_c$  decays based on our estimates for the inclusive rates derived in Sec. IV and on various phenomenological models for the baryonic Isgur-Wise function  $F(\omega)$  entering in the exclusive differential rate, Eq. (3.12). Of all the phenomenological models we

shall mostly focus our attention on the sum rule calculation of [21].

We begin our discussion with the determination of the leading order  $\Lambda_b \rightarrow \Lambda_c$  Isgur-Wise function by the QCD sum rule method given in [21]. The shape of the Isgur-Wise function in [21] can be very well reproduced by an exponential representation of the form

$$F(\omega) = \frac{2}{\omega+1} \exp\left(- (2\rho_B^2 - 1) \frac{\omega-1}{\omega+1}\right), \quad (5.1)$$

which has the correct zero recoil normalization  $F(1) = 1$  and a slope parameter given by  $\rho_B^2$ . The convexity parameter in this representation [proportional to  $(\omega-1)^2$ ] is given by  $c_B = 1/8(-1 + 4\rho_B^2 + 4\rho_B^4)$  and is positive for  $\rho_B^2 \geq 0.207$  as in most model calculations. We refer to this representation of the Isgur-Wise function as the standard form. For the  $\rho_B^2$  parameter the authors of [21] find  $\rho_B^2 = 0.85$  and  $\rho_B^2 = 0.65$  using diagonal and nondiagonal sum rules, respectively. As an average of these two values one obtains

$$\rho_B^2 = 0.75. \quad (5.2)$$

Using the average value of  $\rho_B^2$ ,  $V_{bc} = 0.038$ , the standard representation of the Isgur-Wise function (5.1) and the rate formula (3.12) from Sec. III one obtains the exclusive rate  $\Gamma^{\text{excl}} = 5.52 \times 10^{10} \text{ s}^{-1}$ . From the inclusive rate calculated using the mass parameters given in [19]  $\Gamma^{\text{incl}} = 6.50 \times 10^{10} \text{ s}^{-1}$  one finds  $R_E = 0.85$  for the exclusive/inclusive ratio. Note that the  $V_{bc}$  dependence drops out in this ratio. The values of the slope parameter  $\rho_B^2$  and the exclusive/inclusive ratio  $R_E$  of the model of [21] as well as those of other phenomenological models have been collected together in Table I. Table I uses the larger value of the two inclusive reference rates discussed in Sec. IV based on the mass parameters of [19]. If one instead uses the inclusive rate of [20], all  $R_E$  values in Table I have to be increased by 4.3%. Radiative corrections do not affect the exclusive/inclusive ratios listed in Table I very much since they lower both the exclusive and inclusive rates (see Secs. III and IV). If they were left, out the exclusive/inclusive ratio  $R_E$  would be reduced by  $\approx 2\%$ .

It is clear from Table I that the form factor calculated in the quark confinement model [22] is too flat to satisfy the bound  $\Gamma^{\text{excl}} \leq \Gamma^{\text{incl}}$ . All other models in Table I satisfy this upper bound. Translating the upper bound  $R_E = 1$  into a lower bound on the slope parameter  $\rho_B^2$  one obtains

$$(\rho_B^2)_{\text{min}} = 0.36 \quad (5.3)$$

using the standard form factor function (5.1) and the inclusive rate calculated from the mass parameters in [19].

An upper bound on the slope parameter  $\rho_B$  can be obtained using the spectator model bound discussed in Sec. II, which reads

$$\rho_B^2 \leq 2\rho_M^2 - \frac{1}{2}. \quad (5.4)$$



TABLE I. Predictions of the slope parameter  $\rho_B^2$  and the ratio  $R_E = \Gamma^{\text{excl}}/\Gamma^{\text{incl}}$  calculated in different models.

Model	Isgur-Wise function	$\rho_B^2$	$\Gamma^{\text{excl}}/\Gamma^{\text{incl}}$
Quark confinement model [22]	$\frac{\ln(\omega + \sqrt{\omega^2 - 1})}{\sqrt{\omega^2 - 1}}$	0.33	1.02
QCD sum rules [13]	$\sqrt{\frac{2}{\omega + 1}} \exp\left(-0.8 \frac{\omega - 1}{\omega + 1}\right)$	0.65	0.89
QCD sum rules [21] ( $\rho^2 = 0.75$ )	$\frac{2}{\omega + 1} \exp\left(-2\rho^2 - 1\right) \frac{\omega - 1}{\omega + 1}$	0.75	0.85
Simple quark model [23]	$\left(\frac{2}{\omega + 1}\right)^{(1.32 + 0.7/\omega)}$	1.01	0.78
Relativistic three quark model [24]	$\left(\frac{2}{\omega + 1}\right)^{(1.7 + 1/\omega)}$	1.35	0.68
IMF model [7]	$\frac{1}{\omega} \exp\left(-0.7 \frac{\omega - 1}{2\omega}\right) \frac{\int_{-0.7\sqrt{(\omega+1)/(2\omega)}}^{\infty} dy e^{-y^2} \left(y + 0.7 \sqrt{\frac{\omega+1}{2\omega}}\right)}{\int_{-0.7}^{\infty} dy e^{-y^2} (y + 0.7)}$	1.44	0.66
Skyrme model in the large $N_c$ limit [25]	$0.99 \exp(-1.3(\omega - 1))$	1.30	0.63
MIT bag model [26]	$\left(\frac{2}{\omega + 1}\right)^{(3.5 + 1.2/\omega)}$	2.35	0.45

The mesonic slope parameter  $\rho_M^2$  can be extracted from the exclusive semileptonic  $B$  decays [5]. The values are

$$(\rho_M^2)_1 = 0.66 \pm 0.19 \quad \text{from } \bar{B} \rightarrow D l^- \bar{\nu},$$

$$(\rho_M^2)_2 = 0.71 \pm 0.11 \quad \text{from } \bar{B} \rightarrow D^* l^- \bar{\nu}, \quad (5.5)$$

with the world average values for  $V_{cb}$  being  $|V_{cb}| = 0.0394 \pm 0.0050$  and  $|V_{cb}| = 0.0387 \pm 0.0031$ , respectively. The weighted averages of the two mesonic slope parameters are then  $\rho_M^2 = 0.70 \pm 0.10$ . This translates into an upper bound for the baryonic slope parameter  $\rho_B^2$  according to the spectator quark model bound (5.4). One has

$$(\rho_B^2)_{\text{max}} = 0.89 \pm 0.19. \quad (5.6)$$

We mention that very likely the error on this bound will be considerably reduced in the near future with the new data expected from the bottom quark factories at SLAC and KEK. Combining both limits, Eqs. (5.3) and (5.6), we obtain a prediction for the allowed values of the baryon slope parameter given by

$$0.36 < \rho_B^2 < 0.89 \pm 0.19. \quad (5.7)$$

According to these upper and lower bounds the first model (as remarked on before) and the last four models in Table I have to be excluded since they possess form factors which are too flat or too steep, respectively. The two QCD sum rule calculations [13,21] as well as the simple quark model evaluation [23] feature slope parameters that satisfy the bounds (5.7). We consider the two QCD sum rule calculations to be

the most reliable of the three model calculations since they are the least model dependent. Our final prediction for the range of values of the exclusive/inclusive ratio will be based on the two slope parameter values  $\rho_B^2 = 0.85$  and  $0.65$ , resulting from the analysis of the diagonal and nondiagonal [21] sum rules in [21], respectively. This range also includes the sum rule result of [13]. In determining our prediction for the range of  $R_E$  we shall also allow for the smaller inclusive rate calculated by the method of [20]. Thus our final prediction for the range of the exclusive/inclusive ratio in semileptonic  $\Lambda_b \rightarrow \Lambda_c$  decays is  $R_E = 0.81 - 0.92$ . This range is consistent with the range of values from the semiquantitative analysis performed in Sec. II. Our conclusion is that the exclusive/inclusive ratio of semileptonic  $\Lambda_b$  decays is considerably higher than in the corresponding bottom meson case.

## VI. MISSING FINAL STATES

In addition to the quasielastic  $\Lambda_b \rightarrow \Lambda_c$  contribution discussed before there are also  $\Lambda_c^{**}$  resonant states and multiparticle final states contributing to the fully inclusive semileptonic  $\Lambda_b$  rate. Of course, if the quasielastic contribution dominates the total inclusive rate much more than by the 66% in the heavy meson case, there would not be much room left for the resonant and multiparticle final states. In the main body of this paper we have collected together theoretical evidence that the latter situation is very likely the case. One could turn this statement around in the following sense: if one would have theoretical reasons to believe that resonant

and multiparticle final states are suppressed in inclusive semileptonic  $\Lambda_b \rightarrow X_c$  transitions, then the quasielastic exclusive  $\Lambda_b \rightarrow \Lambda_c$  contribution must dominate. As we shall see there are theoretical reasons to believe in such a suppression inasmuch as some of the transitions to orbitally excited  $\Lambda_c^{**}$  charm baryon states involve spin-orbit coupling transitions which are believed to be suppressed.

The purpose of this section is to classify those final states in semileptonic  $\Lambda_b \rightarrow X_c$  transitions that form the complement of the quasielastic  $\Lambda_b \rightarrow \Lambda_c$  transition. We divide these into class *A* contributions  $\Lambda_b \rightarrow \Lambda_c X l \nu$ , where the charm quark of the decay ends up in a charm  $\Lambda_c$  directly or indirectly, and class *B* contributions, where the charm quark goes into a meson or a charm-strangeness baryon  $\Lambda_b \rightarrow X_c(\text{non-}\Lambda_c)l\nu$ . Accordingly we define the two ratios

$$R_A = \frac{\Gamma(\Lambda_b \rightarrow \Lambda_c X l \nu)}{\Gamma(\Lambda_b \rightarrow X_c l \nu)} \quad (6.1)$$

and

$$R_B = \frac{\Gamma(\Lambda_b \rightarrow X_c(\text{non-}\Lambda_c)l\nu)}{\Gamma(\Lambda_b \rightarrow X_c l \nu)}. \quad (6.2)$$

Together with the exclusive/inclusive ratio defined before,

$$R_E = \frac{\Gamma(\Lambda_b \rightarrow \Lambda_c l \nu)}{\Gamma(\Lambda_b \rightarrow X_c l \nu)}, \quad (6.3)$$

the three ratios must add up to one, i.e.,

$$R_E + R_A + R_B = 1. \quad (6.4)$$

Note that all three ratios are positive definite which makes the constraint (6.4) potentially quite powerful if  $R_E$  is close to 1 as is indicated by our analysis of the quasielastic rate in the previous sections. As concerns the sizes of  $R_A$  and  $R_B$  one cannot even hope to provide semiquantitative answers at present. It is nevertheless useful to enumerate the final states belonging to the class *A* and class *B* transitions which we shall do in the following.

#### A. Class A final states

Potentially prominent among the class *A* final states are the transitions into the seven excited *P*-wave  $\Lambda_c^{**}$  states. Taking the bottom meson case for comparison theoretical estimates show that the corresponding transitions into excited mesonic *P*-wave states make up approximately 10% of semileptonic *B* decays [27]. The  $\Lambda_c^{**}$  states eventually decay down to the  $\Lambda_c$  ground state via (multiple) pion emission or, with a much smaller branching fraction, via photon emission. There are altogether seven such *P*-wave states which are grouped into the three HQS doublets  $\{\Lambda_{cK1}\}$ ,  $\{\Lambda_{ck1}\}$ ,  $\{\Lambda_{ck2}\}$ , and the singlet  $\{\Lambda_{ck0}\}$ . We use the terminology of [2] such that the excited *K* and *k* states are symmetric and antisymmetric under the exchange of the momenta of the light quarks. The five symmetric states  $\{\Lambda_{ck0}\}$ ,  $\{\Lambda_{ck1}\}$ , and  $\{\Lambda_{ck02}\}$  are made from a heavy quark and a light spin-1 diquark.  $\Lambda_b$  transitions into these five states involve spin-0 to

spin-1 light-side transitions which can be expected to be strongly suppressed since they involve spin-orbit interactions. In the spectator quark model, where one neglects spin-orbit interactions, transitions into these five states are forbidden [28]. It would be interesting to experimentally confirm this suppression. One thus remains with the transitions into the HQS doublet  $\{\Lambda_{cK1}\}$  whose spin-1/2<sup>-</sup> and spin-3/2<sup>-</sup> members are very likely the recently discovered  $\Lambda_c(2593)$  and  $\Lambda_c(2625)$  states [1].  $\Lambda_b$  branching ratios into these states are not yet available. There could also be transitions into higher orbital  $\Lambda_c^{**}$  states. These transitions are, however, expected to be suppressed because of angular momentum suppression factors. Besides, transitions into symmetric higher orbital  $\Lambda_c^{**}$  states would again be suppressed due to spin-orbit coupling suppression. The suppression of transitions into the symmetric orbitally excited  $\Lambda_c^{**}$  states could be the source of the possible depletion of class *A* final states. For example, using spin counting, only 1/3 of the existing *P*-wave excitations can be reached in semileptonic  $\Lambda_b$  transitions if the spin-orbit coupling suppression is active.

Another source of class *A* final states is accessible due to the creation of one or more additional (*d* $\bar{d}$ )- or (*u* $\bar{u}$ )-quark pairs in the basic transition. The relevant transitions for (*d* $\bar{d}$ ) creation are [see Fig. 3(a)]

$$\Lambda_b^0 \rightarrow \Lambda_c^+(\Sigma_c^+) + X_M^0 + l^- + \bar{\nu}_l, \quad (6.5)$$

or, when exchanging the *d* ↔ *u* lines originating from the  $\Lambda_b$ , one has

$$\Lambda_b^0 \rightarrow \Sigma_c^0 + X_M^+ + l^- + \bar{\nu}_l. \quad (6.6)$$

For (*u* $\bar{u}$ ) creation shown in Fig. 3(b) one has

$$\Lambda_b^0 \rightarrow \Sigma_c^{++} + X_M^- + l^- + \bar{\nu}_l. \quad (6.7)$$

The exchange of the *d, u* lines originating from the  $\Lambda_b$  brings one back to Eq. (6.5). Here  $X_M$  stands for a charmless mesonic inclusive state. Excited charm baryon states such as  $\Lambda_c^{**}$  and  $\Sigma_c^{**}$  are not explicitly included in the listing (6.5–6.7), but are implied. The  $\Sigma_c^0$ ,  $\Sigma_c^+$ , and  $\Sigma_c^{++}$  appearing in

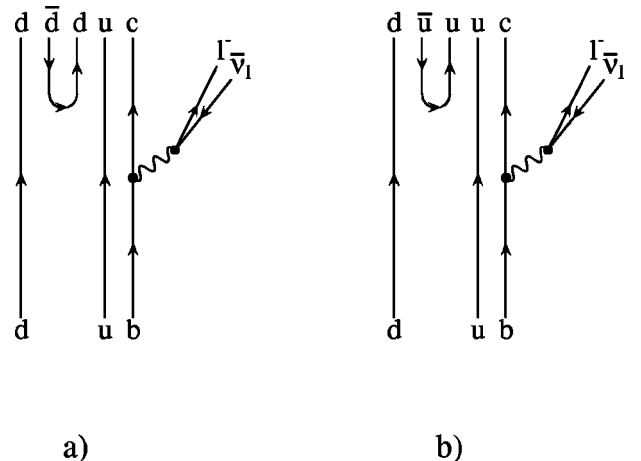
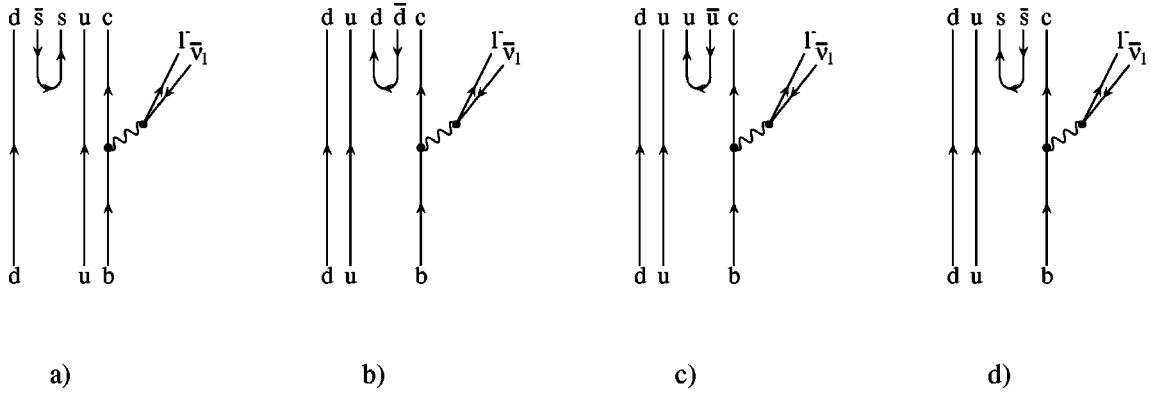


FIG. 3. Class A final states.

FIG. 4. Class  $B$  final states.

Eqs. (6.5–6.7) cascade down to the  $\Lambda_c^+$  state via pion emission, making these processes class  $A$  final states.

### B. Class $B$ final states

There are two sources for class  $B$  final states. First there is  $(s\bar{s})$ -quark pair creation where the strange quark ends up in a charm-strangeness baryon [Fig. 4(a)] which decays weakly into noncharm states and therefore does not contribute to the class  $A$  final states.<sup>3</sup> Second, the charm quark of the decay may end up in a charm meson accompanied by  $(u\bar{u})$ -,  $(d\bar{d})$ -, and  $(s\bar{s})$ -quark pair creation as shown in Figs. 4(b)–4(d). Let us list a few examples of such transitions. From  $(s\bar{s})$  pair creation one has [Fig. 4(a)]

$$\Lambda_b^+ \rightarrow \Xi_c^+ + X_{M_s}^0 + l^- + \bar{\nu}_l \quad (6.8)$$

or, when exchanging the  $d \leftrightarrow u$  lines, one has

$$\Lambda_b^+ \rightarrow \Xi_c^0 + X_{M_s}^+ + l^- + \bar{\nu}_l. \quad (6.9)$$

$X_{M_s}$  now stands for a strangeness meson state. Then there are the transitions where the charm quark goes into a charm meson. These are

$$\Lambda_b^+ \rightarrow D^+ + X_B^0 + l^- + \bar{\nu}_l, \quad (6.10)$$

$$\Lambda_b^+ \rightarrow D^0 + X_B^+ + l^- + \bar{\nu}_l, \quad (6.11)$$

$$\Lambda_b^+ \rightarrow D_s^+ + X_{B_s}^0 + l^- + \bar{\nu}_l. \quad (6.12)$$

$X_B$  stands for a light baryon state and  $X_{B_s}$  for a strangeness baryon state. Excitations of the charm meson and charm baryon states are again implied. We do not discuss  $(c\bar{c})$  pair

<sup>3</sup>The weak decay  $\Xi_c \rightarrow \Lambda_c + \pi$ , though interesting, occurs only at the per mill level [29].

creation. The corresponding final states are barely accessible in semileptonic  $\Lambda_b$  decays for kinematical reasons and will have a spectacular signature anyhow.

## VII. SUMMARY AND CONCLUSION

We have brought together various pieces of theoretical evidence that the exclusive/inclusive ratio  $R_E$  in semileptonic  $\Lambda_b$  decays is larger than in semileptonic  $B$  decays, where the exclusive/inclusive ratio amounts to 66%. We predict that the exclusive quasielastic semileptonic  $\Lambda_b$  decays make up between 81% and 92% of the total inclusive semileptonic  $\Lambda_b$  rate. At present there is no experimental information on either the exclusive or the inclusive branching ratio in semileptonic  $\Lambda_b$  decays. The problem is that present and planned experiments do not have access to reliable  $\Lambda_b$  tags which are necessary for a measurement of their branching fractions. Ideally one would run a  $e^+e^-$  machine right above  $\Lambda_b \bar{\Lambda}_b$  threshold which would solve the tagging problem. However, such experiments are not planned in the foreseeable future. The above assertion about the dominance of the quasielastic mode in semileptonic  $\Lambda_b$  decays may take a long time to verify experimentally. It may nevertheless be used as a working hypothesis in the experimental analysis of semileptonic  $\Lambda_b$  decays in particular if further theoretical progress in the theoretical description of semileptonic  $\Lambda_b$  decays confirms the estimates made in this paper.

## ACKNOWLEDGMENTS

This investigation was prompted by two questions of our experimental colleagues P. Roudeau and G. Sciolla who asked us about theoretical expectations for the size of the the  $\Lambda_c + X$  (class  $A$ ) and  $(\text{non-}\Lambda_c) + X_c$  (class  $B$ ) contributions in inclusive semileptonic  $\Lambda_b$  decays. We did our best to try and provide answers to these questions in our paper, at least partially. We would like to thank N. Uraltsev for fruitful discussions. We also thank O. Yakovlev who participated in the early stages of this calculation. The work of B.M. was partially supported by the Ministry of Science and Technology of the Republic of Croatia under the contract 00980102.

- [1] Particle Data Group, C. Caso *et al.*, Eur. Phys. J. C **3**, 1 (1998).
- [2] J. G. Körner, M. Krämer, and D. Pirjol, Prog. Part. Nucl. Phys. **33**, 787 (1994).
- [3] DELPHI Collaboration, D. Bertini *et al.*, Report No. DELPHI 97-17 PHYS 673, 1997.
- [4] M. A. Ivanov, J. G. Körner, V. E. Lyubovitskij, and A. G. Rusetsky, Phys. Rev. D **59**, 074016 (1999).
- [5] P.S. Drell, CLNS-97-1521, talk given at the 18th International Symposium on Lepton-Photon Intereactions (LP97), Hamburg, Germany, 1997, in “Hamburg 1997—Lepton-Photon Interactions,” pp. 347–378.
- [6] M. Neubert and V. Rieckert, Nucl. Phys. **B382**, 97 (1992).
- [7] B. König, J. G. Körner, M. Krämer, and P. Kroll, Phys. Rev. D **56**, 4282 (1997).
- [8] R. N. Faustov and V. O. Galkin, Z. Phys. C **66**, 119 (1995).
- [9] M. A. Ivanov, J. G. Körner, V. E. Lyubovitskij, and A. G. Rusetsky, Phys. Lett. B **476**, 58 (2000).
- [10] J. G. Körner and M. Krämer, Phys. Lett. B **275**, 495 (1992).
- [11] M. Neubert, Nucl. Phys. **B371**, 149 (1992).
- [12] J. E. Paschalis and G. J. Gounaris, Nucl. Phys. **B222**, 473 (1983).
- [13] Y. B. Dai, C. S. Huang, M. Q. Huang, and C. Liu, Phys. Lett. B **387**, 379 (1996).
- [14] T. Mannel, Phys. Rev. D **50**, 428 (1994); A. Falk and M. Neubert, *ibid.* **47**, 2965 (1993); M. Shifman, N. G. Uraltsev, and A. Vainshtein, *ibid.* **51**, 2217 (1995).
- [15] J. G. Körner and D. Pirjol, Phys. Lett. B **334**, 399 (1994).
- [16] A. F. Falk and M. Neubert, Phys. Rev. D **47**, 2982 (1993).
- [17] Y. Nir, Phys. Lett. B **221**, 184 (1989).
- [18] E. Bagan, P. Ball, V. Braun, and G. Gosdzinsky, Phys. Lett. B **342**, 496 (1995).
- [19] A. A. Penin and A. A. Pivovarov, Nucl. Phys. **B549**, 217 (1999).
- [20] A. H. Hoang, Z. Ligeti, and A. V. Manohar, Phys. Rev. D **59**, 074017 (1999).
- [21] A. G. Grozin and O. I. Yakovlev, Phys. Lett. B **285**, 254 (1992). The numerical evaluation of the sum rules in this published version is erroneous. The error is corrected in the archive version hep-ph/9908364. We would like to thank A.G. Grozin for informing us about the above numerical error.
- [22] G. V. Efimov, M. A. Ivanov, N. B. Kulimanova, and V. E. Lyubovitskij, Z. Phys. C **54**, 349 (1992); D. Ebert, T. Feldmann, C. Kettner, and H. Reinhardt, *ibid.* **71**, 329 (1996).
- [23] B. Holdom, M. Sutherland, and J. Mureika, Phys. Rev. D **49**, 2359 (1994).
- [24] M. A. Ivanov, J. G. Körner, V. E. Lyubovitskij, and P. Kroll, Phys. Rev. D **56**, 348 (1997).
- [25] E. Jenkins, A. Manohar, and M. B. Wise, Nucl. Phys. **B396**, 38 (1996).
- [26] M. Sadzikowski and K. Zalewski, Z. Phys. C **59**, 667 (1993).
- [27] S. Veseli and M. G. Olsson, Phys. Rev. D **54**, 886 (1996).
- [28] F. Hussain, J. G. Körner, J. Landgraf, and S. Tawfiq, Z. Phys. C **69**, 655 (1996).
- [29] M. B. Voloshin, Phys. Lett. B **476**, 297 (2000); S. Sinha and M. P. Khanna, Mod. Phys. Lett. A **14**, 651 (1999).